Transitions to Improved Core Electron Heat Confinement Triggered by Low Order Rational Magnetic Surfaces in the Stellarator TJ-II

T. Estrada 1), D. López-Bruna 1), F. Medina 1), E. Ascasíbar 1), R. Balbín 1), A. Cappa 1), F. Castejón 1), A.A. Chmyga 2), S. Eguilior 1), L. Eliseev 3), A. Fernández 1), J. Guasp 1), C. Hidalgo 1), L. Krupnik 2), A.V. Melnikov 3), S. Petrov 4)

1) Laboratorio Nacional de Fusión, EURATOM-CIEMAT, 28040 Madrid, Spain
2) Institute of Plasma Physics, NSC KIPT , 310108 Kharkov, Ukraine
3) Institute of Nuclear Fusion, RNC Kurchatov Institute, Moscow, Russia
4) A. F. Ioffe Physical Technical Institute, St. Petersburg, Russia

e-mail contact of main author: teresa.estrada@ciemat.es

Abstract. Transitions to improved core electron heat confinement are triggered by low order rational magnetic surfaces in TJ-II ECH plasmas. Experiments are performed changing the magnetic shear around the rational surface n/m=3/2 to study the influence of the island width on the transition, and ECH power modulation is used to look at transport properties. The improvement in the electron heat confinement shows no obvious dependence on the magnetic shear. Transitions triggered by the rational surface n/m=4/2 show an increase in the ion temperature synchronized with the increase in the electron temperature. Ion temperature changes had not been previously observed either in TJ-II or in any other helical device.

1. Introduction

In stellarator devices, transitions to improved core electron heat confinement are established in conditions of high Electron Cyclotron Heating (ECH) power density and are characterized by peaked electron temperature profiles and large radial electric field in the inner plasma region [1-7]. These transitions have been often referred as Neoclassical or electron Internal Transport Barriers (N-ITB or e-ITB) [1,2,4,6] or as “electron root” feature [3]. Recently, the common characteristics of the transitions to improved core heat confinement observed at four helical devices (CHS, LHD, W7-AS and TJ-II) have been discussed and a new name has been adopted: Core Electron Root Confinement (CERC) [8]. This new name reflects the fact that most of the observations are consistent with a transition to the electron-root solution for the radial electric field that can be explained within the framework of the neoclassical theory. However, some observations, like the influence of low order rational surfaces in the rotational transform profile, are rarely included in neoclassical calculations [9].
The specific characteristics of the stellarator TJ-II, i.e. low magnetic shear and high magnetic configuration flexibility, allow us the control of low order rational surfaces within the rotational transform profile and, therefore, the study of how the magnetic topology affects the core heat confinement. TJ-II experiments show that transitions to CERC can be triggered by positioning a low order rational surface at the plasma core region [6]. Experimentally, a rational surface can be positioned within the plasma by selecting the appropriate magnetic configuration or by the induction of an Ohmic current that modifies dynamically the rotational transform profile during the discharge. As it has been discussed in [7] the rational surface contributes to the outward electron flux that creates a locally strong positive radial electric field. In this way, the transitions are achievable at higher plasma densities, reducing the ECH power per particle (P_{ECH}/n_e) threshold. The characteristics of CERC triggered by the n=3/m=2 rational surface are already described in [6,7] and can be summarized as follows. At the transition, the electron temperature and the plasma potential, measured by HIBP, increase in the plasma core region ($\rho < 0.3$), increasing substantially -in a factor of

three- the radial electric field. These magnitudes remain almost unchanged at outer radii. Measurements of the HIBP beam current indicate that, at the transition, the plasma density profile changes to a slightly more hollow profile. Assuming a constant ECH absorbed power, transport analysis indicates an improvement in the electron heat confinement in the plasma core. Besides, quasi-coherent modes are observed -in ECE and HIBP signals- where the E_rxB shear flows develop at the CERC formation. The mode can exist before or after the CERC phenomenon but vanishes as the barrier is fully developed [10]. Finally, transitions triggered by the 3/2 rational have no effect on the ion temperature. Experiments with different low order rationals (n/m: 3/2, 4/2, 5/3…) have showed a dependence of the threshold density (and also of the confinement improvement) on the order of the rational [11].

In this work we report on experiments performed to study the influence of the island width keeping the order of the rational surface (n/m=3/2) and changing the magnetic shear by the induction of Ohmic current. Besides, the particular characteristics of the transitions triggered by the rational surface n/m=4/2 are described.

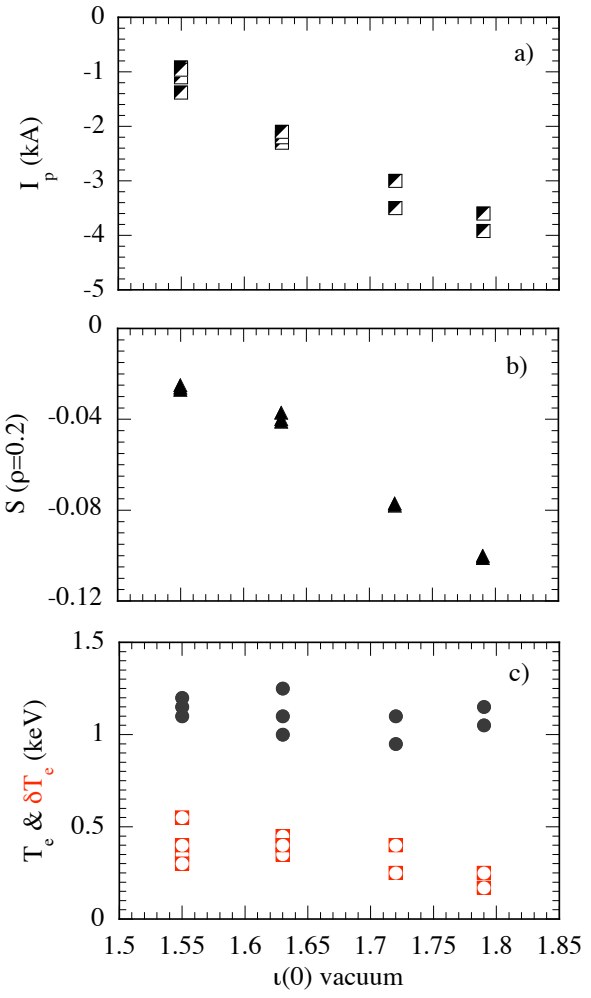

Figure 1: (a) Plasma current required to trigger CERC transition, (b) magnetic shear strength at ρ=0.2 and (c) central T_e before CERC (black) and increase of central T_e at CERC formation (red), as a function of central ι in vacuum.

2. Experimental results

2.1. CERC triggered by n/m=3/2 at various magnetic shear strengths

To study the influence of the island width on the CERC formation while keeping the order of the rational surface, we have performed experiments changing the vacuum magnetic configuration on a shot to shot basis. During each discharge the rotational transform is modified dynamically; the rotational transform decreases and the strength of the negative magnetic shear increases as the induced OH current is driven to more negative values. These experiments have been performed in plasmas with line-averaged densities around 0.5-0.6 10^{19} m^{-3}, heated with ECH at 330 kW (one gyrotron at 80 kW and second one at 250 kW). We observed that the rational 3/2 triggers the CERC formation in configurations with starting vacuum rotational transform at the plasma core from 1.55 to 1.8 at increasing values of the plasma current, from -1 to -4 kA, respectively.

The evolution of the rotational transform profile has been calculated with the ASTRA package [12] considering that the main contribution to the current profile is the induced OH current, assuming Spitzer resistivity corrected by the fraction of

passing particles, and imposing the measured net plasma current evolution as boundary condition. It is expected that the change in magnetic field pitch in the ECH deposition zone makes the parallel refraction index of the heating wave change slightly from the experimental settings (set for no EC current drive). Actually a small amount (but higher the higher OH current) of ECCD has been taken into account.

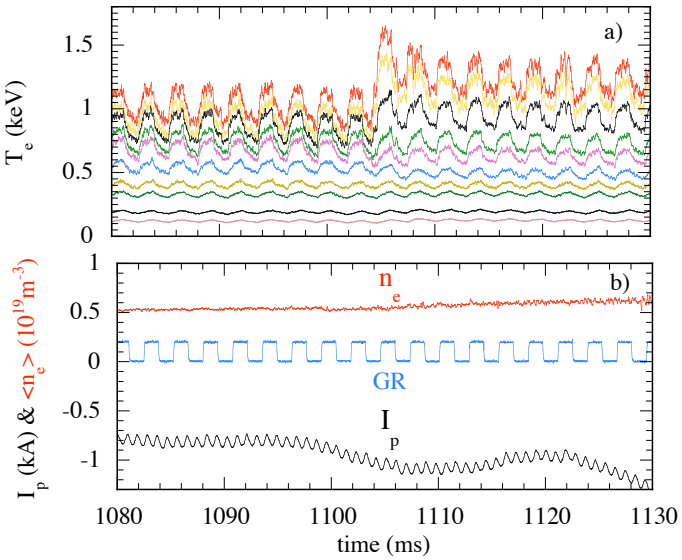

Figure 2: Time evolution of (a) Electron temperature and (b) line density, ECH power and net plasma current. CERC transition is at t=1105 ms.

Figure 1 shows the plasma current required to trigger the transition to CERC (a), the calculated magnetic shear strength at ρ=0.2 when the rational surface 3/2 enters the plasma column (b), and the central electron temperature before CERC and the increase of the electron temperature at CERC formation (c), as a function of rotational transform in vacuum. The increase in the central electron temperature is about 30-35 % in the low magnetic shear cases and drops to 15-20 % as the magnetic shear increases.

In these experiments the ECH power is modulated in order to explore transport properties of plasmas with CERC. The power of one gyrotron is set to 80 kW modulated 100% at a frequency 360 Hz and the power of the other one is kept constant at 250 kW. An example is displayed in figure 2. The time traces of ECE signals at different radial positions show both, the electron temperature profile modulation, and the CERC transition (figure 2.a); the net plasma current and the line-averaged density are shown in figure 2.b, together with the signal of a microwave diode installed in the transmission line of the first gyrotron. Correlation analysis has been done using as reference function the signal of the diode, which is proportional to the modulated power. The cross-correlation function of the ECE signals at different radial positions prior and during CERC is shown in figure 3. The heat pulse propagation velocity decreases between ρ=0.2 and ρ=0.4 (green and blue traces respectively) during CERC, indicating an improvement of the electron heat confinement. The change in the propagation velocity in the radial range ρ: 0.2-0.4 can be also seen in figure 4. It shows the time lag as a function of the radial position without and with CERC. Outside ρ=0.4 the heat pulse

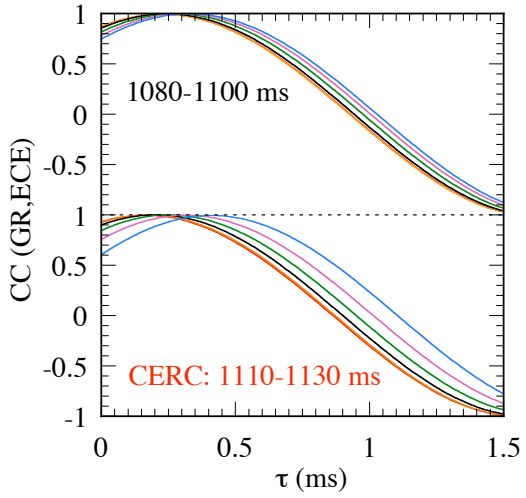

Figure 3: Cross-correlation function between ECH power modulation and ECE signals at different radial locations, prior (top) and during (bottom) CERC. Radial locations: ρ≈0 (red), ρ≈0.2 (green) and ρ≈0.4 (blue).

propagation velocity does not change (the time lag slope is very similar without and with CERC). The difference between the time lag at ρ=0.4 and that at ρ=0.2 is shown in figure 5 as a function of the magnetic shear, prior and during CERC. In all cases the time lag difference increases at the CERC transition, indicating an improvement of the electron heat confinement. Within the accuracy of the experiments, the presence of the island behaves as a switch for the CERC independently of the magnetic shear.

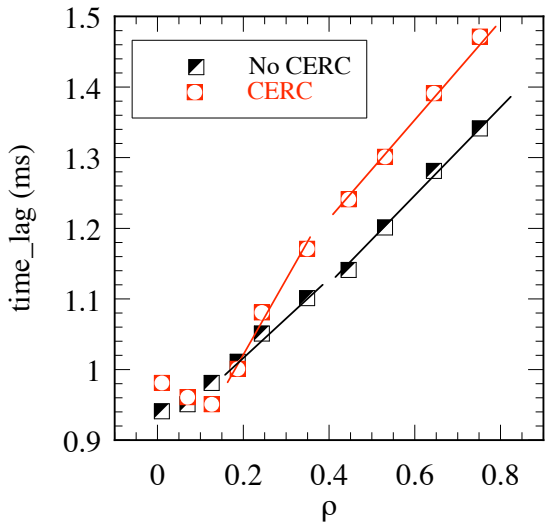

Figure 4: Time lag between ECE signals and ECH power modulation as a function of the radial position, without (black symbols) and with (red symbols) CERC.

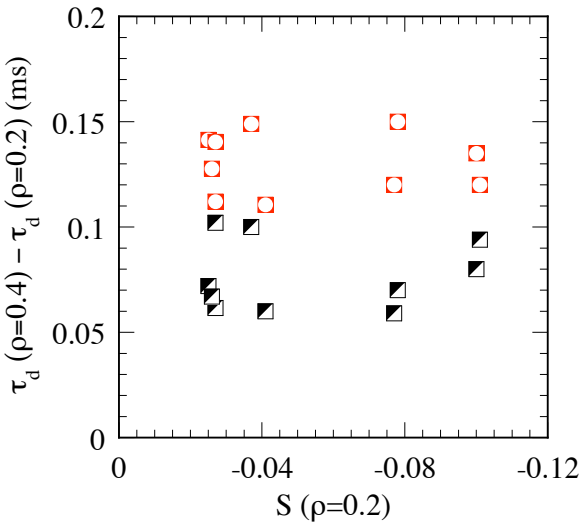

Figure 5: Time lag increment within ρ: 0.2-0.4 as a function of the magnetic shear at ρ=0.2 without (black symbols) and with (red symbols) CERC.

2.2. CERC triggered by n/m=4/2

CERC triggered by the n=4/m=2 rational have been recently studied in TJ-II ECH plasmas. Firstly, it is important to mention that ECH discharges performed in magnetic configurations having the "natural" 4/2 resonance surface in the ι-profile in vacuum show a degraded confinement and very often an unstable evolution. However, the rational 4/2 with moderate magnetic shear can have a favourable effect on the confinement. CERC triggered by the 4/2 rational have been obtained in a magnetic configuration with vacuum rotational transform above two by inducing a small amount of negative current, either ECCD or OH current. This negative current reduces the rotational transform mainly in the inner plasma region, crossing the rational 4/2 with increased negative magnetic shear.

CERC triggered by the 4/2 rational produces an increase in the electron temperature at the plasma centre of about 25% at relatively high line densities: 0.7-0.9 10^{19} m^{-3}. Comparatively, the increase in the central electron temperature in CERC triggered by the 3/2 rational is less pronounced - close to 15% - at similar densities: 0.7-0.8 10^{19} m^{-3}.

Figure 6 shows an example of CERC triggered by the 4/2 rational in a discharge with P_{ECH}=350 kW and in which the plasma current gradually increases due to OH induction. The calculated evolution of the rotational transform profile is shown in figure 6.d. In this example the barrier is formed at about t=1100 ms and it is spontaneously lost and recovered. At the CERC formation, synchronized with the change in the electron temperature, we

observe an increase in the ion temperature measured by CX-NPA diagnostic [13] and a reduction in the H_α signals. As CERC is lost, ECE traces show a heat pulse propagating radially outwards. SXR tomography diagnostic [14] shows a flattening in the profiles localized around $\rho \approx 0.4$ with a m=2 poloidal structure. An example is shown in figure 7. To highlight the poloidal structure of the flattening in the SXR profiles, we have represented in figure 7 (right) the difference between the SXR tomographic reconstructions before and after the transition. This observation together with the absence of quasi-coherent oscillations indicate that in these discharges the magnetic island associated to the "natural" resonance n=4/m=2 does not rotate.

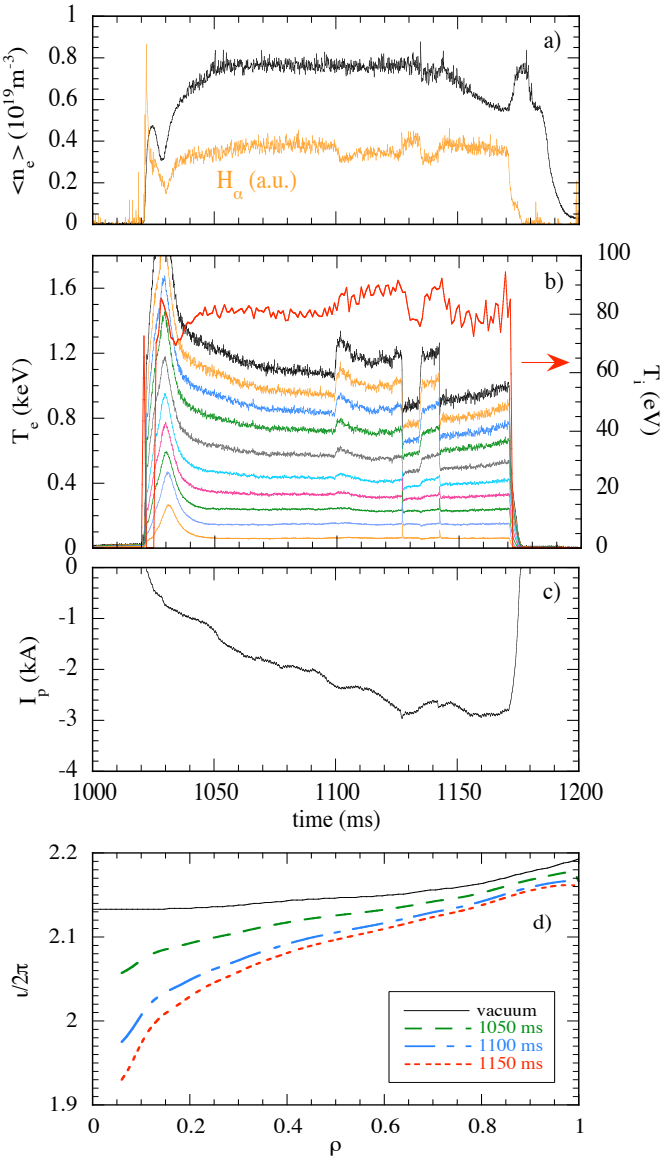

Figure 6: Time evolution of (a) line density and Hα signal, (b) electron temperature at several radii and ion temperature measured along a central plasma chord, and (c) net plasma current; (d) ι-profile at three time instants.

The plasma potential measured using the HIBP diagnostic increases in the central plasma region. However, accurate measurements of plasma potential profiles have not been achieved in this magnetic configuration so far, what has precluded the characterization of the radial electric field rise.

An important result is the increase in the ion temperature synchronized with the increase in the electron temperature (see figure 6.b). The change in the ion temperature is relatively modest (about 10-15 %), but it had not been observed previously either in TJ-II or in the other helical devices [8]. In figure 8 we have represented the ion temperature vs. the central electron temperature of the discharge shown in figure 6. It can be seen that the change in the electron temperature (1 & 3) precedes the change in the ion temperature (2 & 4) during both, CERC formation (1 & 2) and disappearance (3 & 4), being the delay of about 2-3 ms. Outer plasma chords have been scanned with the CX-NPA diagnostic in a series of reproducible discharges. Changes in T_i synchronized with T_e are still visible but lay within the error bars of the CX-NPA diagnostic.

The characteristics of these ECH plasmas, exclude collisional ion heating as the dominant mechanism for the ion temperature change. From power balance calculations we find that the collisional electron-ion power transfer is about 10 kW and it remains almost unchanged as

the CREC develops. The radial electric field increases in transitions triggered by 4/2 or by 3/2, however, the transitions triggered by 3/2 have no effects on T_i. A possible mechanism to explain the ion temperature change would be linked to the resonances of the radial electric field [15,16]. These resonances modify the ion orbits and ion confinement, and the radial electric field needed for them to appear depends strongly on the rotational transform of the magnetic configuration.

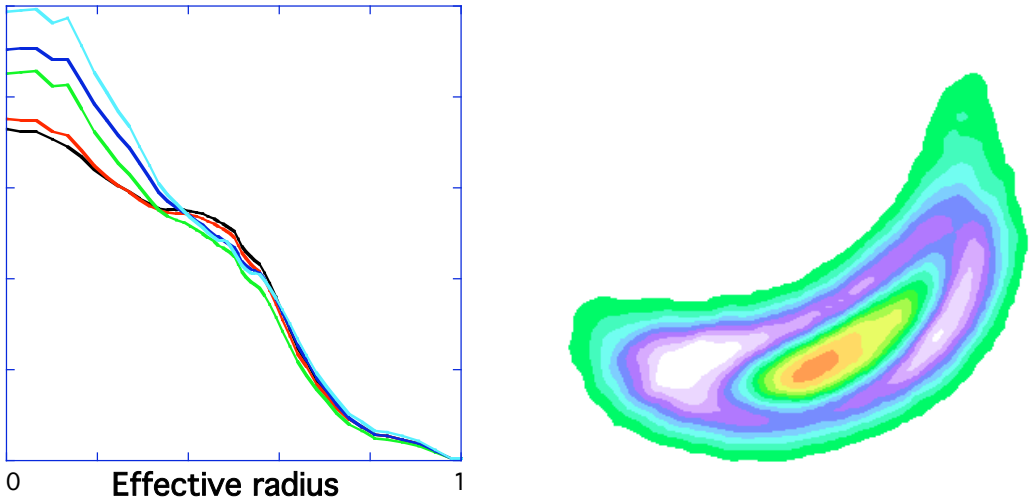

Figure 7: SXR profile evolution (left) and difference between the tomographic reconstruction of the profiles before and during CERC (right).

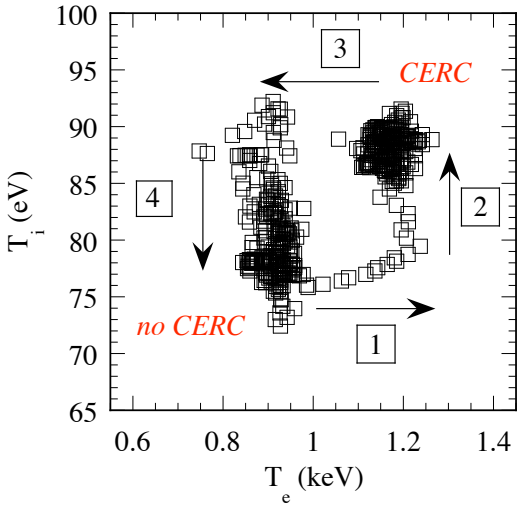

Figure 8: Ion temperature vs. central electron temperature of the discharge shown in fig 6.

3. Conclusions

Experiments have been performed to study the influence of the island width on CERC formation keeping the order of the rational surface (n/m=3/2) and changing the magnetic shear by the induction of Ohmic current. The results indicate that the rational surface n/m=3/2 triggers the transition within the studied range of magnetic shear. In these experiments the ECH power is modulated to explore transport properties of plasmas with CERC. The improvement in the electron heat confinement is reflected by the delay of the heat pulse propagation. The heat confinement improvement is independent of the magnetic shear.

Transitions triggered by the rational surface n/m=4/2 show an increase in the ion temperature synchronized with the increase in the electron temperature. The change in the ion temperature is relatively modest (about 10-15 %) but it had not been observed previously either in TJ-II or in the other helical devices. A possible mechanism to explain the ion

temperature change would be linked to the resonances of the radial electric that modify the ion orbits and ion confinement.

References

[1] FUJISAWA, A., et al., "Electron Thermal Transport Barrier and Density Fluctuation Reduction in a Toroidal Helical System", Phys. Rev. Lett. **82** (1999) 2669
[2] STROTH, U., et al., "Internal Transport Barrier Triggered by Neoclassical Transport in W7-AS", Phys. Rev. Lett. **86** (2001) 5910
[3] MAASSBERG, H., et al., "The Neoclassical Electron Root Feature in the Wendelstein-7-AS Stellarator", Phys. Plasmas **7** (2000) 295
[4] IDA, K., et al., "Characteristics of Electron Heat Transport of Plasma with an Electron Internal Transport Barrier in the Large Helical Device", Phys. Rev. Lett. **91**, 085003 (2003).
[5] CASTEJÓN, F., et al., "Enhanced Heat Confinement in the Flexible Heliac TJ-II", Nuclear Fusion **42** (2002) 271
[6] ESTRADA, T., et al., "Electron Internal Transport Barrier Formation and Dynamics in the Plasma Core of the TJ-II Stellarator", Plasma Phys. Control. Fusion **46** (2004) 277
[7] CASTEJÓN, F., et al., "Influence of Low-order Rational Magnetic Surfaces on Heat Transport in TJ-II Heliac ECRH Plasmas", Nuclear Fusion **44** (2004) 593
[8] YOKOYAMA, M., et al., "Common Features of Core Electron-Root Confinement in Helical Devices", Fusion Science and Technology. *In press*
[9] SHAING, K.C., et al., "Plasma and momentum transport processes in the vicinity of a magnetic island in a tokamak", Nuclear Fusion **43** (2003) 258-261
[10] ESTRADA, T., et al., "Electron Internal Transport Barriers, Rationals and Quasi-Coherent Oscillations in the Stellarator TJ-II", Plasma Phys. Control. Fusion **47** (2005) L57-L63
[11] ESTRADA, T., et al., "Electron Internal Transport Barriers and Magnetic Topology in the Stellarator TJ-II", Fusion Science and Technology **50** (2006) 127-135
[12] PEREVERZEV, G.V., et al., "ASTRA: an Automatic System for Transport Analysis", Max-Planck-Institut für Plasma Physik, Rep. IPP 5142, Garching (1991)
[13] FONTDECABA, J.M., et al., "Energy-Resolved Neutral Particle Fluxes in TJ-II ECRH Plasmas", Fusion Science and Technology **46** (2004) 271
[14] MEDINA, F., et al., "X-ray diagnostic systems for the TJ-II flexible heliac", Rev. Sci. Intrum. 70 (1999) 642
[15] GUASP, J., et al., "Loss cone structure for ions in the TJ-II helical axis stellarator Part I: Properties without a radial electric field", Nuclear Fusion **40** (2000) 411
[16] GUASP, J., et al., "Loss cone structure for ions in the TJ-II helical axis stellarator Part II: Radial electric field effects", Nuclear Fusion **40** (2000) 411